Large change in the exchange interactions of $HgCr_2O_4$ under very high magnetic fields

Shojiro Kimura,[1,*] Masayuki Hagiwara,[1] Tetsuya Takeuchi,[1] Hironori Yamaguchi,[1,†] Hiroaki Ueda,[2,‡] Yutaka Ueda,[2] and Koichi Kindo[2]

[1]*KYOKUGEN, Osaka University, Toyonaka, Osaka 560-8531, Japan*

[2]*Institute for Solid State Physics, University of Tokyo, Kashiwa 277-8581, Japan*

(Received 28 December 2010; revised manuscript received 1 March 2011; published 1 June 2011; publisher error corrected 21 June 2011)

The combination of high-frequency electron magnetic resonance (EMR) and magnetization measurements enables us to evaluate the exchange interactions in high-field phases of polycrystalline samples of the chromium spinel oxide $HgCr_2O_4$. The evaluation indicates that the lattice distortion in this compound largely modulates the exchange interactions between the Cr^{3+} spins to stabilize its distinct plateau with one-half of the saturation magnetization. Furthermore, we show that a release of the lattice distortion occurs in very high magnetic fields. Our result suggests that the spin-lattice coupling, which causes the large changes in the exchange interactions, plays a crucial role in giving rise to the peculiar magnetization process of $HgCr_2O_4$.

DOI: 10.1103/PhysRevB.83.214401 PACS number(s): 75.10.Hk, 75.50.Ee, 76.50.+g

I. INTRODUCTION

In geometrically frustrated antiferromagnets, vast degeneracy prevents the systems from taking a unique ground state. In such systems, a small perturbation away from an ideal model, which causes lifting of the ground state degeneracy, can possibly play a significant role in inducing exotic phenomena. In particular, recent studies revealed that novel types of phase transitions are driven by the coupling of multiple degrees of freedom. Indeed, for chromium spinel oxides ACr_2O_4 ($A = $ Cd and Hg), it has been proposed that a robust 1/2-magnetization plateau is stabilized by the spin-lattice coupling.[1–5] In ACr_2O_4, magnetic Cr^{3+} ions with $S = 3/2$, which have an isotropic Heisenberg-type character with no orbital degeneracy, form a highly frustrated pyrochlore lattice, which is composed of a three-dimensional arrangement of corner sharing tetrahedra. These compounds undergo a transition from a paramagnetic phase with a cubic $Fd\bar{3}m$ crystal symmetry to a magnetically ordered phase with a lower crystal symmetry.[1,2,6] The distinct magnetization plateau appears in their high-field magnetization processes at low temperatures.[1,2] In this paper, from high-field ESR and magnetization measurements, we will show a peculiar behavior where a large change of the exchange interactions due to the spin-lattice coupling occurs to stabilize the plateau in the chromium spinel oxide $HgCr_2O_4$.

Figure 1 shows magnetization curves at different temperatures observed in a polycrystalline sample of $HgCr_2O_4$. The magnetization M increases almost linearly at low fields, but a sudden jump into a plateau phase with a magnetization of one-half of the saturation value occurs around $H_{c1} = 10$ T. The plateau phase terminates at $H_{c2} = 27$ T, and the magnetization smoothly increases above this field. Then, it shows a kink at $H_{c3} = 36$ T with a small hysteresis, and finally the saturation is achieved at around 43 T. In the plateau phase, a peculiar type of symmetry breaking into a collinear ferrimagnetic state with three up and one down spins on each chromium tetrahedron is expected. Theoretical studies have demonstrated that a magnetization plateau can appear owing to a thermal or quantum fluctuation in geometrically frustrated systems.[7,8] However, the plateau due to such a mechanism is only expected to appear in a narrow field and temperature region. On the other hand, in the chromium spinel compounds the plateau is stable in a very wide field and temperature region. A significant feature in the appearance of the plateau for these compounds is that it is accompanied by a deformation of the crystal lattice.[1,9]

Recent diffraction measurements have revealed that the crystal structure in the plateau phase has the same space-group symmetry as the magnetic structure, which is a 16 sublattice ferrimagnetic one with a cubic $P4_332$ symmetry.[9] In this plateau phase, the distance between two Cr^{3+} spins aligning antiparallel to each other is about two percent shorter than the one for spins with a parallel alignment, suggesting that the lattice distortion stabilizes the ferrimagnetic order.[9] In fact, it was also demonstrated that effective theories, which take a magnetoelastic interaction into account, can lead to a wide magnetization plateau.[3–5] The role of the spin-lattice coupling can be summarized as follows: atomic displacements caused by the lattice transformation bring about changes in the exchange interactions resulting in the appearance of the robust magnetization plateau. In this study, we have found that the large changes in the interactions actually occur owing to the lattice transformation in $HgCr_2O_4$. Our analysis shows that the lattice distortion in the 1/2-plateau phase modulates the exchange interactions between the Cr^{3+} spins in such a way that the nearest-neighbor interactions become unequal to stabilize the plateau. Moreover, as the magnetic field further increases above H_{c2}, release of the lattice distortion starts to take place. We suggest continuous changes of the exchange parameters in a field region $H_{c2} < H < H_{c3}$ and a structural transition of a first order at H_{c3}.

II. EXPERIMENTAL PROCEDURES

High-field electron magnetic resonance (EMR) measurements on a polycrystalline sample of $HgCr_2O_4$ have been performed in the frequency region from 75 GHz to 1.4 THz. The measurements in the frequency region from 78 GHz to 1.4 THz in pulsed magnetic fields of up to 55 T at 1.3 K were conducted by using a far-infrared laser, a backward-wave tube, and Gunn oscillators as light sources. Detailed frequency dependencies of the ESR spectrum below 360 GHz in static magnetic fields up to 14 T at 1.6 K were measured by utilizing a vector network analyzer and a

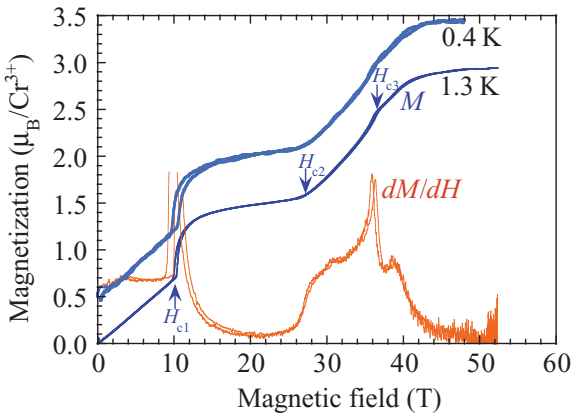

FIG. 1. (Color online) High-field magnetization (M) curves observed at 1.3 and 0.4 K, and the field-differential-magnetization (dM/dH) curve at 1.3 K in $HgCr_2O_4$. The magnetization curve at 0.4 K shifts up by $0.5\mu_B/Cr^{3+}$.

superconducting magnet. The magnetization curves at 1.3 and 0.4 K shown in Fig. 1 were obtained in this study. The result is consistent with the previous report.[2] The magnetization at 0.4 K was measured by utilizing a ^{3}He cryostat. Polycrystalline samples of $HgCr_2O_4$ were prepared by thermal decomposition of Hg_2CrO_4.[2,10,11]

III. RESULTS AND DISCUSSION

Figure 2 shows the EMR spectra observed in a polycrystalline sample of $HgCr_2O_4$. A symmetric line shape of the EMR spectra indicates that the system is highly isotropic. The frequency-field relation of the EMR resonance points is shown in Fig. 3. Vertical dashed lines show H_{c1}, H_{c2}, and H_{c3}. For H_{c1} and H_{c3}, the mean values of the transition fields between field ascending and descending processes are indicated. In the lowest field anitiferromagnetic phase, two kinds of EMR modes, ω_g with a finite zero-field gap and a gapless ω_0, are observed. As the field increases, the ω_g mode approaches the paramagnetic resonance line with $g = 1.97$, determined from the EMR measurements at 150 K, whereas the ω_0 deviates from that. In the plateau phase above H_{c1}, three kinds of EMR modes, ω_+, ω_-, and ω_u, are obtained. The ω_+ with a strong signal intensity is observed at the paramagnetic resonance fields. The ω_- mode has a negative slope and becomes soft at H_{c2}. The ω_u mode has a positive slope with $g = 1.97$ in the 1/2-plateau phase. Above H_{c2}, the slope of this mode, however, changes to negative. At H_{c3}, the resonance frequency of the ω_u mode steeply drops to zero. We analyze the EMR modes based on a molecular-field theory in terms of a four-sublattice model for which the sublattice moments occupy vertices of a single tetrahedron. For the analysis, a Heisenberg-type Hamiltonian $\mathcal{H} = \sum J_{ij}\, \boldsymbol{S}_i \cdot \boldsymbol{S}_j$ with $J > 0$ for an antiferromagnetic interaction is assumed. We take only the nearest-neighbor exchange interaction into account for the analysis because the previous magnetization measurements under high pressure indicated significant dominance of the nearest-neighbor interaction compared to further-neighbor ones.[12] The theoretical ESR modes are obtained from a conventional method by solving equations of motion.[13]

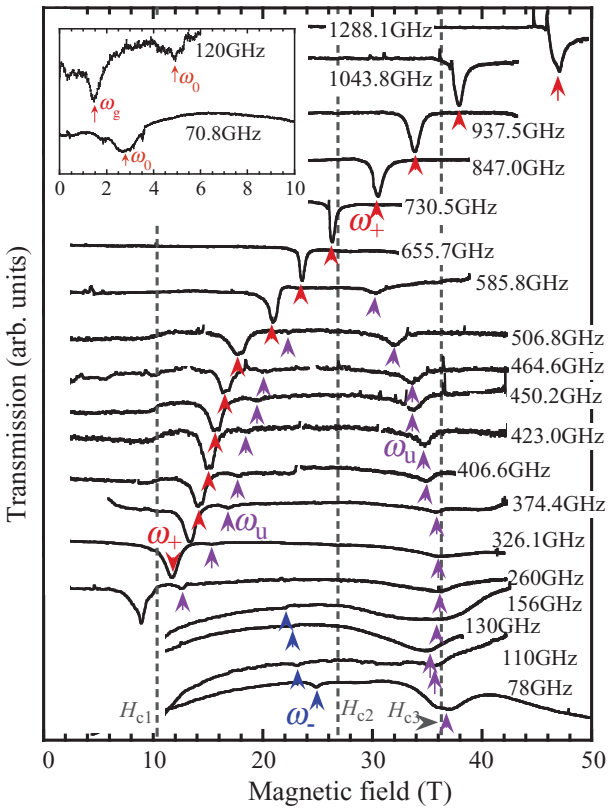

FIG. 2. (Color online) Frequency dependence of EMR spectra observed in pulsed fields at 1.3 K. The dashed vertical lines from left to right indicate H_{c1}, H_{c2}, and H_{c3} respectively. The inset shows extended ESR spectra at 60 and 120 GHz observed in static fields at 1.6 K.

First, we examine the lowest-field phase below H_{c1}. The magnetic structures proposed in this phase are rather complicated, characterized by two kinds of wave vectors.[9] Each tetrahedron in these structure, however, is made up of two up spins and two down spins. Thus we assume a Nèel-type magnetic structure with two up and two down spins for the analysis of this phase. A molecular-field theory, assuming this structure with an easy plane anisotropy, gives two observable EMR modes, expressed as $\hbar\omega_0 = g\mu_B H$ and $\hbar\omega_g = \sqrt{(g\mu_B H)^2 + E_g^2}$ with $E_g = 4\, S\, (J_{AF}\, D)^{1/2}/g\mu_B$. The EMR mode ω_0 and ω_g are expected for the easy plane and for the hard axis, respectively. From the zero-field gap $E_g = 102$ GHz and magnetic susceptibility $\chi = (g\ \mu_B)^2/(8\ J_{AF}) = 0.065\ (\mu_B/\mathrm{T})$, the exchange interaction J_{AF} between spins with antiparallel alignment and the zero-field splitting D term in the antiferromagnetic phase are evaluated to be $J_{AF}/k_B = 5.1$ K and $D/k_B = 0.13$ K. The principal axis of the CrO_6 octahedron in the spinel structure orients along [1 1 1], [1 −1 1], [−1 1 1], or [−1 −1 1] directions. This means that the magnetic principal axis of each Cr^{3+} spin is in a tetramer pointing along four kinds of directions. In such a case, an effective anisotropy, which corresponds to the average of the anisotropy for all the Cr^{3+} sites, is evaluated from the EMR measurements. Since D is small enough compared with J_{AF}, we neglect the anisotropy in the following analysis. It should be mentioned that although the lattice distortion is expected to

cause at least two kinds of nearest-neighbor interactions, our simple analysis can derive only one interaction. Furthermore, the observed deviation of ω_0 from the paramagnetic resonance line can not be explained. For a more detailed discussion of the low-field phase, however, measurements of the single crystal, which unfortunately has not been synthesized so far, are desired.

Next, we discuss the field-induced phases above H_{c1}. In the 1/2-plateau phase we assume a collinear ferrimagnetic state with three up and one down spins on a tetrahedron. We consider that the value of the exchange interaction J_1 between spins aligning antiparallel to each other is different from that of J_2 between spins with parallel alignment because of the difference between the Cr-Cr distances. The details of the molecular-field calculation are described in the Appendix. The calculation gives three kinds of ferrimagnetic resonance modes expressed as follows:

$$\hbar\omega_+ = g\mu_B H, \tag{1}$$

$$\hbar\omega_- = 6J_1 - g\mu_B H, \tag{2}$$

$$\hbar\omega_u = 3(J_1 - 3J_2) + g\mu_B H. \tag{3}$$

Here, the ω_u mode is doubly degenerated. As shown in Fig. 3, the ESR modes observed in the plateau phase can be reproduced by theoretical lines calculated with the parameters of $J_1/k_B = 6.0$ K, $J_2/k_B = 2.5$ K, and $g = 1.97$. This result indicates a significantly large inequality between J_1 and J_2. Above H_{c2}, it is expected that a magnetic structure in which spins are smoothly canted from the collinear ferrimagnetic configuration is realized because the magnetization change at H_{c2} is continuous. Assuming this canted ferrimagnetic structure, the molecular-field calculation gives the ω_+ mode that coincides with the paramagnetic-resonance line as well as

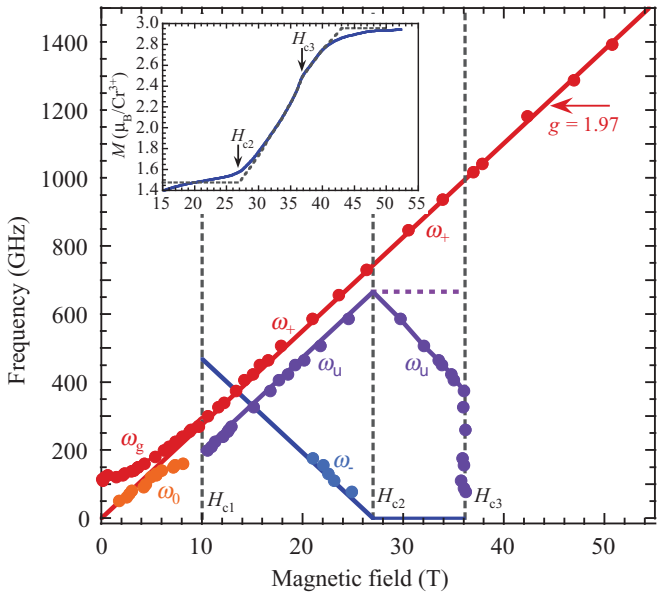

FIG. 3. (Color online) Frequency-field relation of the EMR resonance points. Solid and dotted curves are theoretical ESR modes. Dashed vertical lines show H_{c1}, H_{c2}, and H_{c3}. The inset shows the magnetization curves above the 1/2-magnetization plateau. The solid and dashed curves in the inset are experimental and theoretical results, respectively

with that in the plateau phase, and the ω_- mode turns to be $\omega_- = 0$. These are compatible with the experimental results. The ω_u mode for $H > H_{c2}$, which is given as $\omega_u = 9(J_1 - J_2)$, however, does not agree with the theoretical line calculated with the J_1 and J_2 of the plateau phase. As the field increases, the experimental resonance points for the ω_u mode deviate from the calculated ESR mode, shown by the dotted line in Fig. 3. This fact suggests that the exchange interactions are not the same as those in the plateau region for $H > H_{c2}$. Since ω_u is proportional to the difference between J_1 and J_2, the observed negative slope of the ω_u mode above H_{c2} indicates a decrease in the difference between the exchange interactions as the field increases. Thus, we determine the J_1 and J_2 for $H > H_{c2}$ so as to reproduce the ω_u and the magnetization M, which is given as $M = (g\mu_B)^2 H/(8J_1)$ for a Cr^{3+} ion by assuming the canted ferrimagnetic structure. Figure 4 shows the field dependencies of the exchange interactions obtained by our analysis. This result shows that both J_1 and J_2 are field dependent for $H_{c2} < H < H_{c3}$. At H_{c3}, where the magnetization curve shows a kink, the resonance frequency of the ω_u sharply drops to zero. Therefore, the J_1 and J_2 must become identical at this field. This behavior indicates that a first-order structural transformation to the spinel structure with no distortion takes place at H_{c3}. Above this field, the exchange interaction is evaluated from the analysis of M by assuming a ground-state magnetization of a classical pyrochlore antiferromagnet, which is given by the same expression as for the canted ferrimagnetic state. The analysis indicates a slight decrease in the interaction above H_{c3}. One may consider the crystal structure without lattice distortion to be compatible with a field-induced ferromagnetic structure in which all spins are polarized along the field direction and thus no geometrical spin frustration exists. In the field region above H_{c3}, however, the magnetization shows a further increase. A recent Monte-Carlo simulation for the classical pyrochlore antiferromagnet with an effective biquadratic interaction, which is derived from the magnetoelastic coupling, showed that the magnetization curve before the saturation largely broadens with a slight increase in temperature.[14] Overall the behavior of the experimental

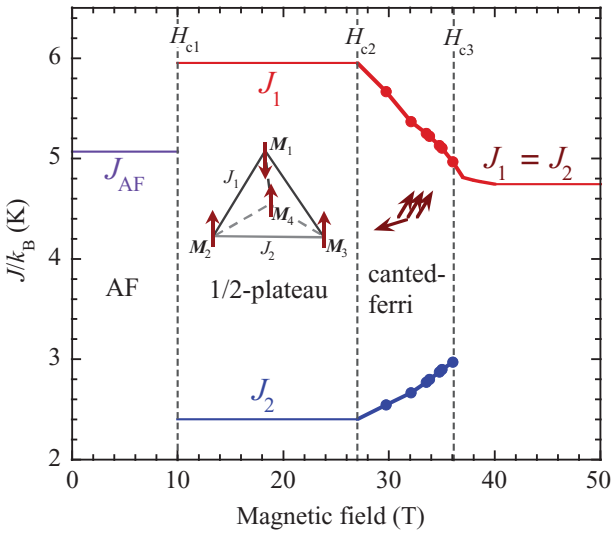

FIG. 4. (Color online) Exchange interactions evaluated from the analysis. Dashed vertical lines show H_{c1}, H_{c2}, and H_{c3}.

magnetization curve, however, does not change between 0.4 and 1.3 K, as shown in Fig. 1. On the other hand, one can find the peak of the differential-magnetization (dM/dH) curve at 38.6 T, suggesting the possibility of existence of another phase between the canted ferrimagnetic and fully polarized phases. We also notice a tiny dM/dH peak around 30 T. These findings show that the magnetization process of $HgCr_2O_4$ is more complicated than that predicted by the theory with the effective biquadratic interaction.[3,4,14]

In the above discussion, we have shown the changes of the exchange interactions in $HgCr_2O_4$ as the magnetic field increases. It is reasonable to consider that these changes are caused by the field-induced structural transformations. Besides the structural transition from the lowest field phase with the orthorhombic $Fddd$ symmetry to the 1/2-plateau phase with the cubic $P4_332$ symmetry at H_{c1},[9] recent synchrotron x-ray diffraction measurements have shown a gradual change in the lattice parameter as the field increases above H_{c2}.[15] The continuous field dependence of the exchange interactions, suggested from our analysis for $H_{c2} < H < H_{c3}$, is consistent with this observation. Our analysis indicated the crucial role of the spin-lattice coupling in the appearance of the robust 1/2 plateau and the release of the lattice distortion in high magnetic fields for $HgCr_2O_4$. For $H > H_{c1}$, the lattice distortion strengthens the exchange interaction J_1 between the spins with antiparallel alignment and weakens the interaction J_2 between the spins with parallel alignment to stabilize the ferrimagnetic structure. Then, in the field region between H_{c2} and H_{c3}, the distortion gradually diminishes as magnetic fields increase, giving rise to the continuous changes of J_1 and J_2. Moreover, our results suggested that the transition to the phase with higher symmetry than $P4_332$ occurs at H_{c3}. The analysis showed that the values of the exchange interactions in $HgCr_2O_4$ largely change owing to the lattice transformation. A large inequality between J_1 and J_2 with the ratio $J_1/J_2 = 2.54$ is evaluated for the plateau phase. On the other hand, it is known that the exchange interactions between Cr^{3+} spins in the chromium spinel compounds are particularly sensitive to the Cr-Cr distance. Actually, substitution of ions on the A site, which causes variation of the lattice constant, causes a considerable change in the Weiss temperature.[1,2,16] The pressure effects on the Weiss temperature also indicated a large enhancement of the antiferromagnetic interaction due to the shrinkage of the Cr-Cr distance.[12] Previous studies demonstrated a dominant contribution from the direct Cr-Cr exchange interaction, which is strongly affected by the Cr-Cr distance, on the nearest-neighbor interaction in the chromium spinel oxides.[12,17–19] $CdCr_2O_4$ with the lattice constant $a = 8.596$ Å has a Weiss temperature $\theta = -70$ K,[1,16] whereas $HgCr_2O_4$ with $a = 8.661$ Å has $\theta = -32$ K (see Ref. 2). Thus a shrinkage in the Cr-Cr distance of one percent is expected to cause an increase in the Weiss temperature by a factor of about two. We believe that about a two percent difference of the Cr-Cr distances in the plateau phase, which was reported from the x-ray diffraction measurements,[9] is enough to cause the large inequality of the exchange interactions evaluated in this study. Finally, we mention a remaining issue in this work. The EMR mode ω_u is, in principle, unobservable owing to the fact that the transverse components of precession motion against the magnetic field of each sublattice cancel each other. The complicated magnetic anisotropy of the spinel compound, in which the magnetic principal axis of each Cr^{3+} spin points along four kinds of directions as mentioned before, might give rise to a finite transition probability. To clarify the reason of why the ω_u mode is observed further detailed theory is desired.

IV. SUMMARY

In conclusion, from the analysis of the EMR modes and magnetization curve based on a molecular-field theory, we have evaluated the exchange interactions of $HgCr_2O_4$ in very high magnetic fields. Our analysis shows that the interactions are largely changed owing to the field-induced lattice transformations, and it indicates a crucial role of the spin-lattice coupling in the appearance of the 1/2 plateau in $HgCr_2O_4$.

ACKNOWLEDGMENTS

This work was partly supported by Grant-in-Aid for Scientific Research (Nos. 17072005 and 20340089) from MEXT and by Global COE Programs (No. G10) from JSPS.

APPENDIX

The EMR modes in the plateau phase are calculated based on a molecular-field theory. In terms of a four-sublattice model, the molecular-field energy is given as

$$\begin{aligned} E = {} & A(\boldsymbol{M}_1\boldsymbol{M}_2 + \boldsymbol{M}_1\boldsymbol{M}_3 + \boldsymbol{M}_1\boldsymbol{M}_4) \\ & + B(\boldsymbol{M}_2\boldsymbol{M}_3 + \boldsymbol{M}_3\boldsymbol{M}_4 + \boldsymbol{M}_4\boldsymbol{M}_2) \\ & - \frac{1}{2}\sum_i \boldsymbol{M}_i\tilde{\Gamma}\boldsymbol{M}_i - \boldsymbol{H}_0\sum_i \boldsymbol{M}_i, \end{aligned} \tag{A1}$$

where $\boldsymbol{M}_1$ is a sublattice moment for down spins, and $\boldsymbol{M}_2$, $\boldsymbol{M}_3$, and $\boldsymbol{M}_4$ are those for up spins. The first and second terms represent the exchange interactions with J_1 and J_2, respectively. Coefficients A and B are expressed by

$$A = \frac{4}{N}\frac{2J_1}{g\mu_B} \tag{A2}$$

and

$$B = \frac{4}{N}\frac{2J_2}{g\mu_B}, \tag{A3}$$

where N is the number of spins, g is the g value, and μ_B is the Bohr magneton. The third term represents a uniaxial anisotropy with a tensor form given by

$$\tilde{\Gamma} = \begin{pmatrix} \Gamma' & 0 & 0 \\ 0 & \Gamma' & 0 \\ 0 & 0 & -2\Gamma' \end{pmatrix}. \tag{A4}$$

The relation between Γ' and the zero-field-splitting (ZFS) D term is given as

$$D = \frac{3g\mu_B\Gamma' M_0}{2S}. \tag{A5}$$

The fourth term represents the Zeeman energy. The EMR resonance conditions are obtained by solving the equation of motion,

$$\frac{1}{\gamma}\frac{\boldsymbol{M}_\mathrm{i}}{dt} = [\boldsymbol{M}_\mathrm{i} \times \boldsymbol{H}_\mathrm{i}], \tag{A6}$$

where $\boldsymbol{H}_\mathrm{i}$ is a molecular field acting on the ith sublattice and is given by

$$\boldsymbol{H}_\mathrm{i} = -\frac{\partial E}{\partial \boldsymbol{M}_0}. \tag{A7}$$

The equation is solved by assuming a precession motion of sublattice moments around the axis parallel to the external magnetic field. For example, in the case of $\boldsymbol{H}_0 \| z$, the following expressions are substituted in the equation:

$$M_\mathrm{i}^{\mathrm{x,y}}(t) = \partial M_\mathrm{i}^{\mathrm{x,y}} e^{\mathrm{i}\omega t}, \tag{A8}$$

$$M_\mathrm{i}^{z} = M_0 = \frac{N}{4} g\mu_\mathrm{B} S, \tag{A9}$$

where $\partial M_\mathrm{i}^{\mathrm{x,y}}$ is a constant. In the case of $D << J$ and $D << g\mu_\mathrm{B}H_0$, which are satisfied in the plateau phase of $HgCr_2O_4$, the EMR modes can be expressed as follows: for $\boldsymbol{H}_0 \| z$

$$\hbar\omega_+ = g\mu_\mathrm{B}H_0 + 6D, \tag{A10}$$

$$\hbar\omega_- = -g\mu_\mathrm{B}H_0 + 6J_1 + 6D, \tag{A11}$$

$$\hbar\omega_\mathrm{u} = g\mu_\mathrm{B}H_0 + 3(J_1 - 3J_2) + 6D, \tag{A12}$$

and for $\boldsymbol{H}_0 \| x, y$

$$\hbar\omega_+ = g\mu_\mathrm{B}H_0 - 3D, \tag{A13}$$

$$\hbar\omega_- = -g\mu_\mathrm{B}H_0 + 6J_1 - 3D, \tag{A14}$$

$$\hbar\omega_\mathrm{u} = g\mu_\mathrm{B}H_0 + 3(J_1 - 3J_2) - 3D. \tag{A15}$$

The obtained EMR modes, which are linear with respect to magnetic fields, are simple. Owing to the magnetic anisotropy, the EMR modes shift an order of D from those of $D = 0$. However, because $D/k_\mathrm{B} = 0.13$ K in $HgCr_2O_4$, it is small enough compared to the exchange interaction so we can neglect the ZFS in our analysis. Thus, even though we use the powder sample, we accomplish a detailed analysis for the plateau phase.

The intensity of the EMR mode is calculated to be proportional to the square of the total amplitude ΔM of the precession motion of the sublattice moment, which is given as

$$\Delta M = \left| \sum_\mathrm{i} \left(\partial M_\mathrm{i}^\mathrm{x} + i M_\mathrm{i}^\mathrm{y} \right) \right|. \tag{A16}$$

$\partial M_\mathrm{i}^{\mathrm{x,y}}$s are obtained by solving the equation of motion. ΔM for the ω_+ mode is calculated as

$$\Delta M \approx 2 + \frac{3D}{J_1} \sim O(1), \tag{A17}$$

whereas for the ω_- mode it is calculated as

$$\Delta M \approx \frac{D}{J_1} \sim O(0.1). \tag{A18}$$

These results explain the observed weak signal intensity of the ω_- mode. In the case of the ω_u mode, the total amplitude ΔM is calculated to be zero because the amplitudes of the precession motion $\partial M_\mathrm{i}^{\mathrm{x,y}}$ for each sublattice cancel each other. Such an ESR mode is, in principle, unobservable. On the other hand, the observed signal of the ω_u mode is weak but finite. The reason why the ω_u mode becomes observable is, however, not clear at the moment. The EMR modes for the canted ferrimagnetic structure are obtained by solving the transposed equation of motion:

$$\frac{1}{\gamma}\frac{d\boldsymbol{M}'_\mathrm{i}}{dt} = \tilde{R}_\mathrm{i}\left[\left(\tilde{R}_\mathrm{i}^{-1}\boldsymbol{M}'_\mathrm{i}\right) \times \left(\tilde{R}_\mathrm{i}^{-1}\boldsymbol{H}'_\mathrm{i}\right) \right]. \tag{A19}$$

Here, $\tilde{R}_\mathrm{i}$ is a matrix that transposes the coordinates such that the equilibrium direction of the magnetization of each sublattice corresponds to the z axis. $\tilde{R}_\mathrm{i}$ is given as

$$\tilde{R}_\mathrm{i} = \begin{pmatrix} \cos\theta_\mathrm{i} & 0 & -\sin\theta_\mathrm{i} \\ 0 & 1 & 0 \\ \sin\theta_\mathrm{i} & 0 & \cos\theta_\mathrm{i} \end{pmatrix}, \tag{A20}$$

where θ_i ($i = 1$–4) is an angle between the direction of the ith sublattice moment and the direction of the external field. M'_i and H'_i are the ith sublattice moment and the molecular field on this moment expressed by new coordinates. The angle θ_i is determined by the following equilibrium conditions that minimize the free energy:

$$\sin\theta_1 = 3\sin\theta_{2,3,4} \tag{A21}$$

and

$$AM_0(\cos\theta_1 + 3\cos\theta_{2,3,4}) = g\mu_\mathrm{B}H_0. \tag{A22}$$

After calculating the equilibrium directions of the sublattice moments, we obtain the resonance conditions for the canted ferrimagnetic structure as follows:

$$\hbar\omega_+ = g\mu_\mathrm{B}H_0, \tag{A23}$$

$$\hbar\omega_- = 0, \tag{A24}$$

$$\hbar\omega_\mathrm{u} = 9(J_1 - J_3). \tag{A25}$$

In the calculation for the canted ferrimagnetic structure we neglected the ZFS term.

*shkimura@imr.tohoku.ac.jp; present address: Institute for Materials Research, Tohoku University, 2-1-1 Katahira, Sendai 980-8577, Japan.

†Present address: College of Integrated Arts and Science, Osaka Prefecture University, Sakai 588-8531, Japan.

‡Present address: Department of Chemistry, Graduate School of Science, Kyoto University, Kyoto 606-8502, Japan.

[1] H. Ueda, H. A. Katori, H. Mitamura, T. Goto, and H. Takagi, Phys. Rev. Lett. **94**, 047202 (2005).

[2] H. Ueda, H. Mitamura, T. Goto, and Y. Ueda, Phys. Rev. B **73**, 094415 (2006).

[3] K. Penc, N. Shannon, and H. Shiba, Phys. Rev. Lett. **93**, 197203 (2004).

[4] K. Penc, N. Shanon, Y. Motome, and H. Shiba, J. Phys. Condens. Matter **19**, 145267 (2007).

[5] D. L. Bergman, R. Shindou, G. A. Fiete, and L. Balents, Phys. Rev. B **74**, 134409 (2006).

[6] Y. Kino and B. Luthi, Solid State Commun. **9**, 805 (1971).

[7]H. Kawamura and S. Miyashita, J. Phys. Soc. Jpn. **54**, 4530 (1985).
[8]D. L. Bergman, R. Shindou, G. A. Fiete, and L. Balents, Phys. Rev. Lett. **96**, 097207 (2006).
[9]M. Matsuda, H. Ueda, A. Kikkawa, Y. Tanaka, K. Katsumata, Y. Narumi, T. Inami, Y. Ueda. and S.-H. Lee, Nat. Phys. **3**, 397 (2007).
[10]H. A. Dabkowska, J. Cryst. Growth **54**, 607 (1981).
[11]A. L. Wessels, R. Czekalla, and W. Jeitschenko, Mater. Res. Bull. **33**, 95 (1998).
[12]H. Ueda and Y. Ueda, Phys. Rev. B **77**, 224411 (2008).
[13]S. Foner, *Magnetism I*, ed. G. T. Rado and H. Suhl (Academic, New York, 1963).
[14]Y. Motome, K. Penc, and N. Shannon, J. Magn. Magn. Mater. **300**, 57 (2006).
[15]Y. Tanaka, Y. Narumi, N. Terada, K. Katsumata, H. Ueda, Y. Staub, K. Kindo, T. Fukui, T. Yamamoto, R. Kammuri, M. Hagiwara, A. Kikkawa, Y. Ueda, H. Toyokawa, T. Ishikawa, and H. Kitamura, J. Phys. Soc. Jpn. **76**, 043708 (2008).
[16]P. K. Baltzer, P. J. Wojtowicz, M. Robbins, and E. Lopatin, Phys. Rev. **151**, 367 (1966).
[17]A. B. Sushkov, O. Tchernyshyov, W. Ratcliff, S. W. Cheong, and H. D. Drew, Phys. Rev. Lett. **94**, 137202 (2005).
[18]R. Valdès Aguilar, A. B. Sushkov, Y. J. Choi, S. W. Cheong, and H. D. Drew, Phys. Rev. B **77**, 092412 (2008).
[19]A. N. Yaresko, Phys. Rev. B **77**, 115106 (2008).